

Original Article

RING-finger protein 6 enhances c-Myc-mediated Warburg effect by promoting MAD1 degradation to facilitate pancreatic cancer metastasis

Yumin Qiu^{1*}, Hengqing Zhu^{1*}, Debin Xu^{1*}, Qian Feng¹, Chongyu Wen¹, Yunyan Du², Mingfeng Xiang³, Leifeng Chen¹, Xiaogang Peng⁴

¹Department of General Surgery, The Second Affiliated Hospital of Nanchang University, Nanchang 330006, Jiangxi Province, China; ²Department of Medical, Jiangxi Provincial People's Hospital of Nanchang University, Nanchang 330006, Jiangxi Province, China; ³Department of Urology, The Second Affiliated Hospital of Nanchang University, Nanchang 330006, Jiangxi Province, China; ⁴Jiangxi Province Key Laboratory of Molecular Medicine, The Second Affiliated Hospital of Nanchang University, Nanchang 330006, Jiangxi Province, China. *Equal contributors.

Received December 25, 2020; Accepted March 22, 2021; Epub May 15, 2021; Published May 30, 2021

Abstract: Aerobic glycolysis (the Warburg effect) promotes tumor metastasis; hence, drugs targeting its regulators are being developed. c-Myc, a critical transcription factor that regulates the Warburg effect, is involved in the tumorigenesis of many cancers, including pancreatic cancer (PC). However, the upstream regulating mechanisms of c-Myc in PC are unclear. Herein, we reported that E3 ubiquitin ligase RING-finger protein 6 (RNF6) was upregulated in PC tissues, and an elevated RNF6 level was closely associated with metastasis and poor prognosis in patients with PC. In functional experiments, RNF6 over-expression accelerated the metastatic ability of PC cells, whereas RNF6 knockdown impaired PC cell motility and invasiveness along with metastasis in an orthotopic mouse model. Furthermore, we found that RNF6 promoted PC cell metastasis by enhancing c-Myc-mediated aerobic glycolysis. Mechanistically, RNF6 increased the expression level of c-Myc by catalyzing the ubiquitination of Max-dimerization protein-1 (MAD1), a cellular antagonist of c-Myc. Lastly, RNF6 promoted the degradation of MAD1 via the ubiquitin-proteasome pathway, and this reduction in the MAD1 levels enabled c-Myc to promote the Warburg effect in PC. Our results demonstrate that RNF6 may be a novel biomarker in PC carcinogenesis, thereby indicating that targeting the RNF6/MAD1/c-Myc axis is a potential strategy for PC therapy.

Keywords: Pancreatic cancer, RNF6, Warburg effect, metastasis, c-Myc, MAD1

Introduction

Pancreatic cancer (PC) is one of the most fatal malignancies worldwide, and its incidence is increasing annually, especially in industrialized countries [1]. Despite recent improvements in PC diagnosis and therapy, the 5-year survival rate of patients with PC has remained dismal (as low as 6%) [2]. A high rate of metastasis is the leading causes of therapy failure in patients with PC according to an autopsy series, which reported that distant metastasis occurs in 90% of cases [3, 4]. Therefore, the identification of novel approaches or targets is urgently required for improving treatment to prevent distal metastasis of PC.

Aerobic glycolysis, also known as the Warburg effect, is a shift from oxidative phosphorylation to glycolysis and is considered to be the root of the occurrence and development of tumors [5]. An enhanced Warburg effect is a fundamental property of many human cancers, including PC [6]. In particular, the metastatic ability of PC has been shown to be closely correlated with enhanced aerobic glycolysis [7]. Protooncogene c-Myc is an important transcription factor that regulates the process of glycolysis, which directly mediates the expression of genes involved in the regulation of glucose metabolism [8, 9]. Increasing evidence shows that c-Myc plays a key role in the tumorigenesis of many tumors [10], including those of PC [11].

RNF6 facilitates pancreatic cancer metastasis

Although the deregulation of c-Myc contributes to PC progression and aerobic glycolysis, the upstream regulating mechanisms of c-Myc remains unclear.

It has been reported that oncogene proteins are regulated by the ubiquitin-proteasome system (UPS). As a substrate interaction module, E3 ubiquitin ligases, have been attracting increasing attention [12]. RING-finger protein 6 (RNF6), a RING-domain E3 ubiquitin Ligase, mediates the ubiquitination of its target proteins and tags them for proteasomal degradation [13, 14]. A large number of studies have shown that *RNF6* functions as an oncogene in multiple cancers such as hepatocellular carcinoma [15], esophageal squamous cell carcinoma [16] and prostate cancer [17]. Additionally, high RNF6 level is an indicator of poor prognosis for colorectal cancer [18, 19]. Importantly, we observed elevated RNF6 mRNA in pancreatic cancer tissues through the Cancer Genome Atlas (TCGA) dataset, which was analysed using GEPIA software (<http://gepia.cancer-pku.cn/>) (Figure S1). These data suggest that RNF6 may play a role in pancreatic cancer tumorigenesis and development. However, the molecular function of RNF6, its target protein substrates, and its clinical significance in PC are unclear.

In this study, we aimed to determine the role of RNF6 in the progression of PC. We further explored the mechanisms of c-Myc overexpression in PC and found that RNF6 positively regulates c-Myc expression by destabilising Max dimerisation protein 1 (MAD1), a key antagonist of c-Myc [20]. Our work identified an interplay among these proteins that promotes PC metastasis by enhancing the Warburg effect.

Materials and methods

Clinical specimens

Matched cancerous and normal pancreatic tissue specimens were obtained from 109 patients with PC admitted to the Second Affiliated Hospital of Nanchang University from 2015 to 2019. Written informed consent was obtained from all patients, and the research procedure was approved by the Ethics and Research Committees of the Second Affiliated Hospital of Nanchang University. All specimens from resection surgery were frozen and stored at -80°C for further analysis. The clinical characteristics of all patients are summarised in **Table 1**.

Over-expression constructs, shRNA plasmids, and cell transfection

Vectors encoding RNF6, c-Myc, or MAD1 and plasmids encoding short hairpin RNAs (shRNAs) against either RNF6 or MAD1 were synthesised by GenePharma (Shanghai, China). PC cells were transfected with these overexpression constructs or shRNA plasmids using Lipofectamine 3000 (Invitrogen, USA) according to the manufacturer's instructions.

In vivo metastasis assay

The nude mice (male BALB/c-nu/nu, 6-8 weeks old) were purchased from the Animal Center of Nanjing Medical University. 5×10^5 PC cells were stably transduced with firefly luciferase gene and injected into the tail vein of BALB/c nude mice. After 6-8 weeks, for *in vivo* signal detection, the mice were anesthetized with isoflurane and then imaged in a Lumina Series III IVIS instrument (PerkinElmer, USA). Then, the mice were euthanized, and their lungs were removed and stained with haematoxylin and eosin stain (H&E) for pathological examination. The animal work was approved by the Ethics Committee for Animal Experiments of the Second Affiliated Hospital of Nanchang University.

Extracellular acidification rate (ECAR) and oxygen consumption rate (OCR)

Metabolic profiles were tested using the Glycolysis Stress Test and Mito Stress Test Kits using the Seahorse XFe96 Analyser according to the manufacturer's instructions.

Mass spectrometry

PC cell lysates were collected and immunoprecipitated with RNF6 antibodies or IgG. Next, the bound proteins were resolved via sodium dodecyl sulfate-polyacrylamide gel electrophoresis (SDS-PAGE), visualised using Coomassie blue staining, and then subjected to mass spectrometric analysis. Proteins were identified by comparing their sequences with those on the human RefSeq protein database.

Co-immunoprecipitation (Co-IP) and in vivo ubiquitination assay

Co-IP assays were performed as described previously [21]. For the *in vivo* ubiquitination assay, RNF6-overexpressing or RNF6-silenced

RNF6 facilitates pancreatic cancer metastasis

Table 1. Correlation between RNF6 and clinicopathologic characteristics of 109 PAAD patients

Variables	clinicopathological characteristics	numbers	RNF6 high expression	RNF6 low expression	<i>p</i> value
Age	<60	45	28	17	0.764
	≥60	64	38	26	
Gender	Female	49	30	19	0.896
	Male	60	36	24	
Tumor site	Pancreatic head	64	37	27	0.485
	Pancreatic body and tail	45	29	16	
Tumor size	<3 cm	40	21	19	0.19
	≥3 cm	69	45	24	
Histologic grade	High differentiation	51	23	28	0.002**
	Middle and low differentiation	58	43	15	
TNM stage	I-II	49	20	29	<0.001***
	III-IV	60	46	14	
Lymph node metastasis	Negative	65	34	31	0.032*
	Positive	44	32	12	
Vessel invasion	NO	60	27	33	<0.001***
	YES	49	39	10	
CEA	Normal	25	14	11	0.596
	Abnormal	84	52	32	

* $P < 0.05$, ** $P < 0.01$, *** $P < 0.001$.

PC cells were treated with MG132 for 4 h before being harvested. Then, the cell lysate was immunoprecipitated with anti-MAD1 antibodies, and the ubiquitination level of MAD1 was tested with an anti-Ub antibody. In addition, to detect MAD1 ubiquitination in HEK293 cells, the cells were transfected with Flag-MAD1, His-RNF6, and HA-Ub constructs and further incubated with MG132 (15 μ M). To assess the MAD1 ubiquitination type, MAD1 mutants (mutations of all lysine residues) and two Ub mutants (K48R and K63R) were purchased from GenePharma.

Statistical analysis

All data were expressed as mean \pm standard errors of means using GraphPad Prism 6 (GraphPad Software, USA). Significant differences were analysed using the Student's *t*-test

and two-tailed distributions. The Kaplan-Meier method was used to calculate the survival curve, and log-rank test was used to determine the significance. $P < 0.05$ was considered significant. Other materials and methods are provided in the [Supplementary Data](#).

Results

High expression of RNF6 is closely associated with metastasis and poor prognosis of patients with PC

To investigate the role of RNF6 in PC, we detected the RNF6 expression level in PC tissues and compared it with that in the adjacent normal tissues. As shown in **Figure 1A** and **1B**, aberrant RNF6 expression occurred in PC tissues, whereas a weak positive signal was detected in corresponding normal tissues. In

RNF6 facilitates pancreatic cancer metastasis

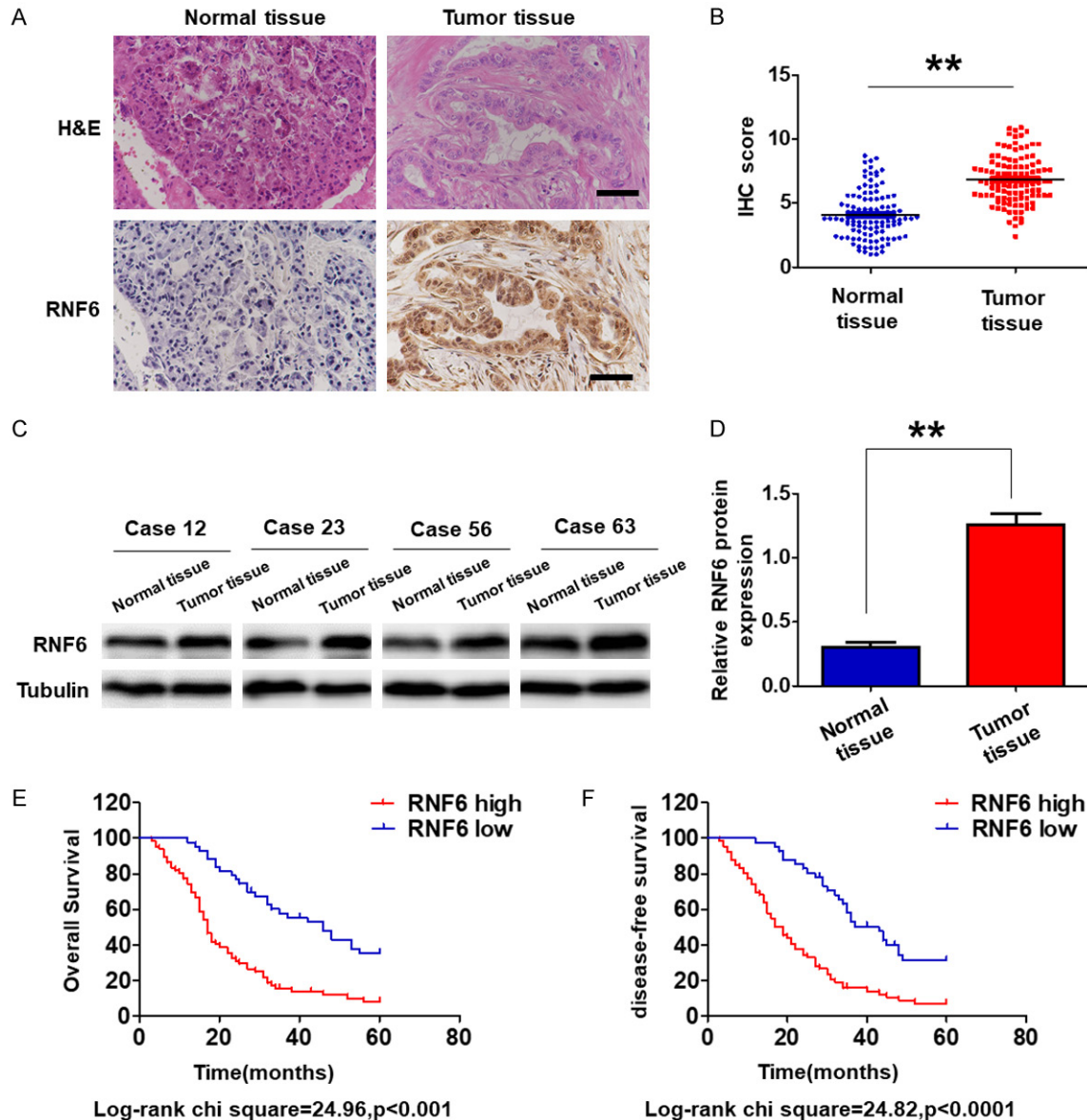


Figure 1. High RNF6 level correlates with poor prognosis in PC patients. (A and B) Representative image (A) and quantification (B) of IHC staining of RNF6 in PC tissues and paired normal tissues. The image was captured at 400 \times magnification. Scale bar, 50 μ m. ** $P < 0.01$. (C and D) Determination and quantification of RNF6 protein levels in PC tissues and paired normal tissues by western blotting assay. Tubulin was used as a loading control. ** $P < 0.01$. (E and F) Kaplan-Meier plots representing probabilities of progression-free and overall survival in 109 PC patients according to expression level of RNF6. Statistical analysis was conducted using Student's t-test and Log Rank test.

keeping with the IHC results, the western blot data showed that RNF6 protein expression was remarkably higher in PC tissues than in normal pancreatic tissues (Figure 1C and 1D). These results revealed that RNF6 is highly expressed in PC, suggesting that it may be involved in the progression of PC.

To determine the pathologic significance of RNF6 expression in PC progression, we anal-

ysed the correlation between RNF6 expression and established PC prognostic factors (Table 1). No significant association was observed between RNF6 expression with age, sex, or tumour size in PC patients. However, RNF6 overexpression was significantly correlated with histologic grade ($P = 0.002$), TNM stage ($P < 0.001$), lymph node metastasis ($P < 0.001$) and vessel invasion ($P = 0.032$). As shown in Figure 1E and 1F, shorter overall survival (OS)

RNF6 facilitates pancreatic cancer metastasis

Table 2. Univariate and multivariate analyses of overall survival in PC patients

Parameters	Univariate analysis			Multivariate analysis		
	HR	95% CI	P value	HR	95% CI	P value
Age (≥ 60 vs < 60)	1.374	0.628-3.165	0.764	-	-	-
Sex (Female vs Male)	1.773	0.509-2.845	0.896	-	-	-
Tumor site (head vs body and tail)	1.668	0.737-2.665	0.485	-	-	-
Tumor size (< 3 vs ≥ 3)	1.672	0.643-4.215	0.190	-	-	-
CEA (Normal vs Abnormal)	1.212	0.643-1.976	0.596	-	-	-
Histologic grade (High vs Middle/Low)	1.329	1.759-4.324	0.002*	1.553	1.248-2.375	0.031*
TNM stage (I-II vs III-IV)	2.908	1.835-5.522	$< 0.001^*$	1.834	1.459-5.332	0.008*
Lymph node metastasis (No vs Yes)	1.569	1.134-3.452	0.032*	1.764	1.365-3.897	0.013*
Vessel invasion (No vs Yes)	1.213	1.132-2.243	$< 0.001^*$	1.224	0.976-2.214	0.067
RNF6 expression (High vs Low)	3.513	2.216-6.432	0.003*	2.981	1.611-5.332	0.009*

HR, hazard ratio; CI, confidence interval; * $P < 0.05$.

and disease-free survival (DFS) in the high level of RNF6 expression group than those in the low level of RNF6 expression group were observed in our cohort of PC patients. Additionally, the results of multivariate Cox regression analysis indicate that RNF6 overexpression predicted shorter OS and RFS in PC patients (**Table 2**), supporting that high RNF6 level is an independent risk factor for PC progression.

RNF6 promotes PC cell migration and invasion in vitro, and metastasis in vivo

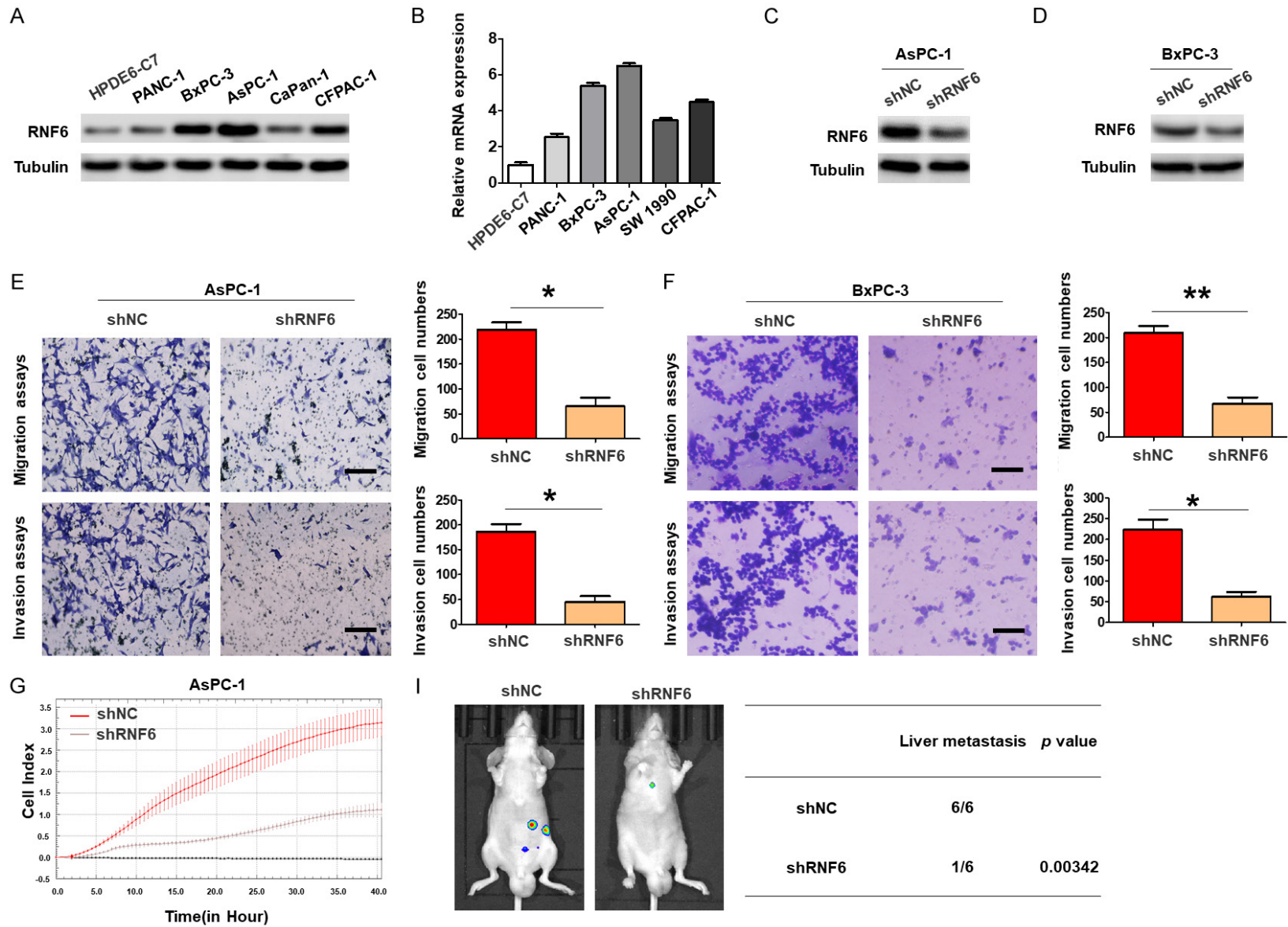
To evaluate the impact of RNF6 expression on PC biology, we transfected two PC cell lines exhibiting high endogenous RNF6 expression (AsPC-1 and BxPC-3) with shRNF6 plasmids to knock down their RNF6 expression (**Figure 2A-D**). Migration and invasion assays indicated that RNF6 silencing significantly suppressed the mobility and invasiveness of PC cells (**Figure 2E** and **2F**). Consistently, the data of RTCA assays also shown that RNF6 knock-down obviously inhibited the metastasis ability of AsPC-1 and BxPC-3 cells (**Figure 2G** and **2H**). Conversely, we infected PANC-1 and CaPan-1 cells, which have intermediate levels of endogenous RNF6 expression, with vectors containing RNF6 (**Figure S2A** and **S2B**). We found that RNF6 upregulation promoted PANC-1 and CaPan-1 cell migration and invasion (**Figure S2C** and **S2D**). RTCA assays demonstrated that RNF6 overexpression enhanced the migratory activity of both PC cell lines, more so than that of control cells (**Figure S2E** and **S2F**).

Next, we determined the effect of altered RNF6 expression on PC metastasis *in vivo*. As shown in **Figure 2I**, the *in vivo* tumor metastatic assay revealed that knockdown of RNF6 rescued the decreased incidence of liver metastasis. Additionally, H&E-stained serial liver sections revealed that RNF6 silencing markedly suppressed experimental liver metastasis (**Figure 2J**). However, overexpression of RNF6 increased liver metastasis (**Figure S2G** and **S2H**). These data clearly demonstrate that RNF6 promotes the invasion and metastasis of PC cells *in vitro* and *in vivo*, indicating that RNF6 might function as an oncogene for PC.

The Warburg effect is crucial for the oncogenic functions of RNF6

To determine the mechanism by which RNF6 influences the invasion and metastasis of PC, we applied RNA-Seq to find global changes in the transcriptome when RNF6 was knocked down in AsPC-1 cells. KEGG analysis revealed that the top downregulated gene set in RNF6-knockdown cells was associated with glycolysis (**Figure 3A**). Therefore, we assessed whether RNF6 could modulate the glycolytic phenotype in PC cells. As expected, RNF6 silencing reduced glucose uptake, lactate production and ATP generation in AsPC-1 and BxPC-3 cells (**Figures 3B-D**, **S3A-C**). Further, RNF6 knock-down also suppressed the extracellular acidification rate (ECAR), which indicated overall glycolytic flux (**Figures 3E**, **S3D**). We also examined OCR (cellular oxygen consumption rate), an indicator of mitochondrial respiration. RNF6-silenced PC cells displayed an increase in OCR (**Figures 3F**, **S3E**). In contrast, RNF6 overex-

RNF6 facilitates pancreatic cancer metastasis



RNF6 facilitates pancreatic cancer metastasis

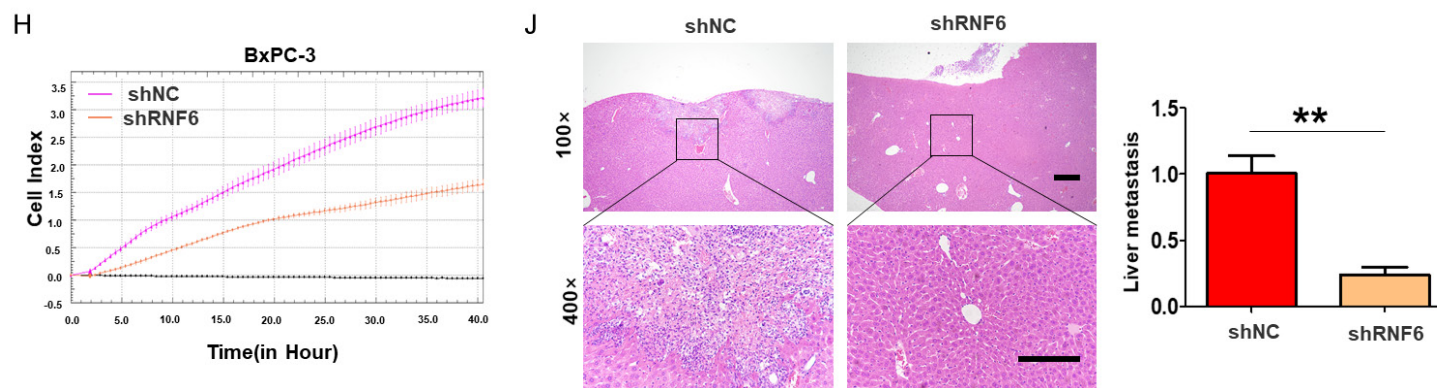
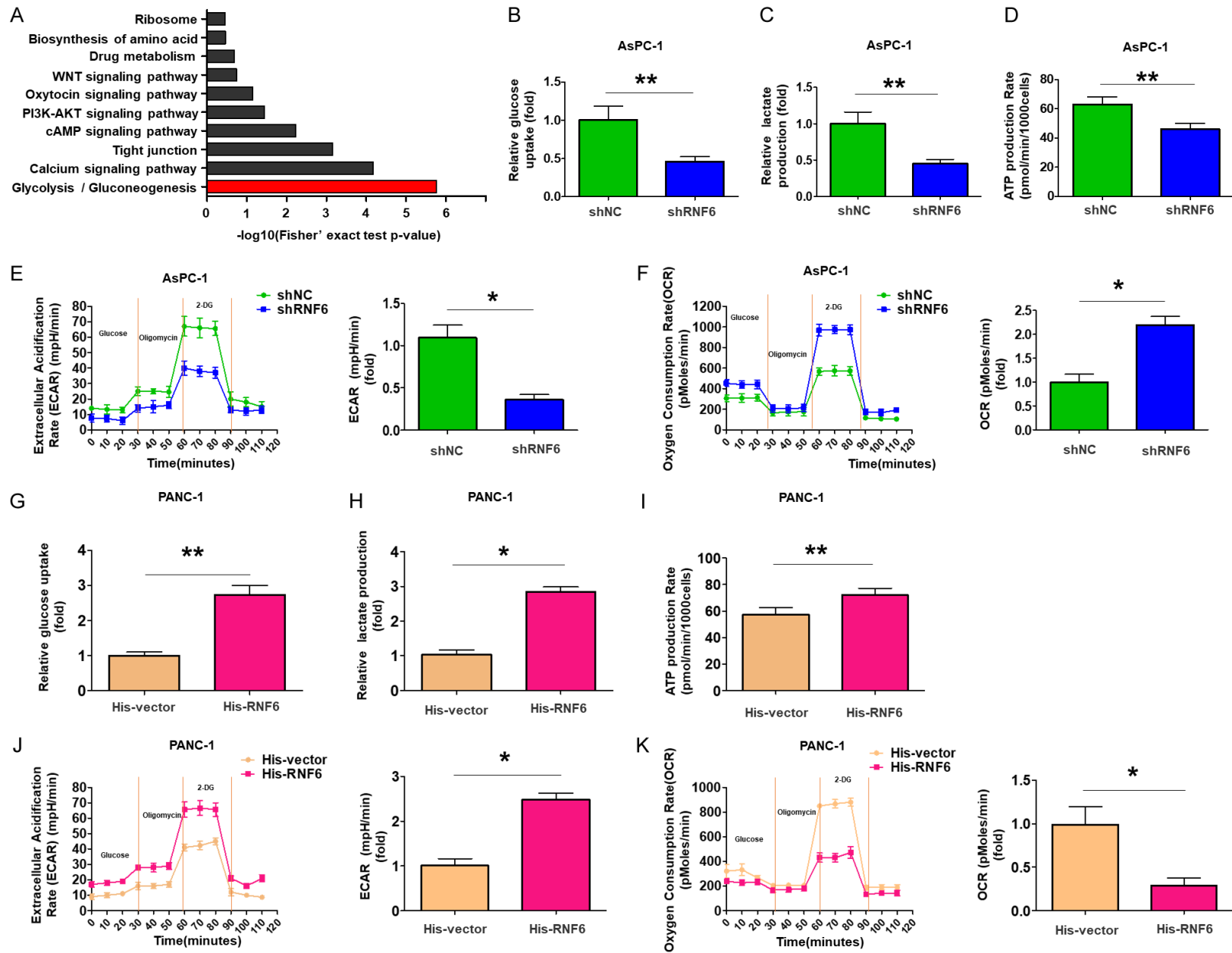


Figure 2. RNF6 promotes migration and invasion of PC cell *in vitro* and accelerates the metastasis of PC cell *in vivo*. A and B. The protein and mRNA levels of RNF6 were detected in four PC cells and the immortalised H6c7 line. Tubulin was used as a loading control. C and D. Western blot analyses were used to detect the expression level of RNF6 in AsPC-1 and BxPC-3 cells stably transfected with the RNF6-silenced vector. Tubulin was used as a loading control. E and F. Transwell migration and Transwell invasion assays of AsPC-1 and BxPC-3 cells transfected with RNF6 knockdown vector. The image was captured at 400 \times magnification. Scale bar, 50 μ m. * P <0.05, ** P <0.01. G and H. RTCA assays were performed to detect the metastasis ability of AsPC-1 and BxPC-3 cells transfected with RNF6-knockdown vector. I. BxPC-3/shRNF6 cells were injected into the tail vein of nude mice, and the incidence of liver metastasis were measured after 6-8 weeks. n=6, ** P <0.01. J. Representative image (left; magnification: \times 100, inset magnification: \times 400) and quantification (right) of H&E staining of liver metastatic nodules. n=6/group. Scale bar, 50 μ m. ** P <0.01.

RNF6 facilitates pancreatic cancer metastasis



RNF6 facilitates pancreatic cancer metastasis

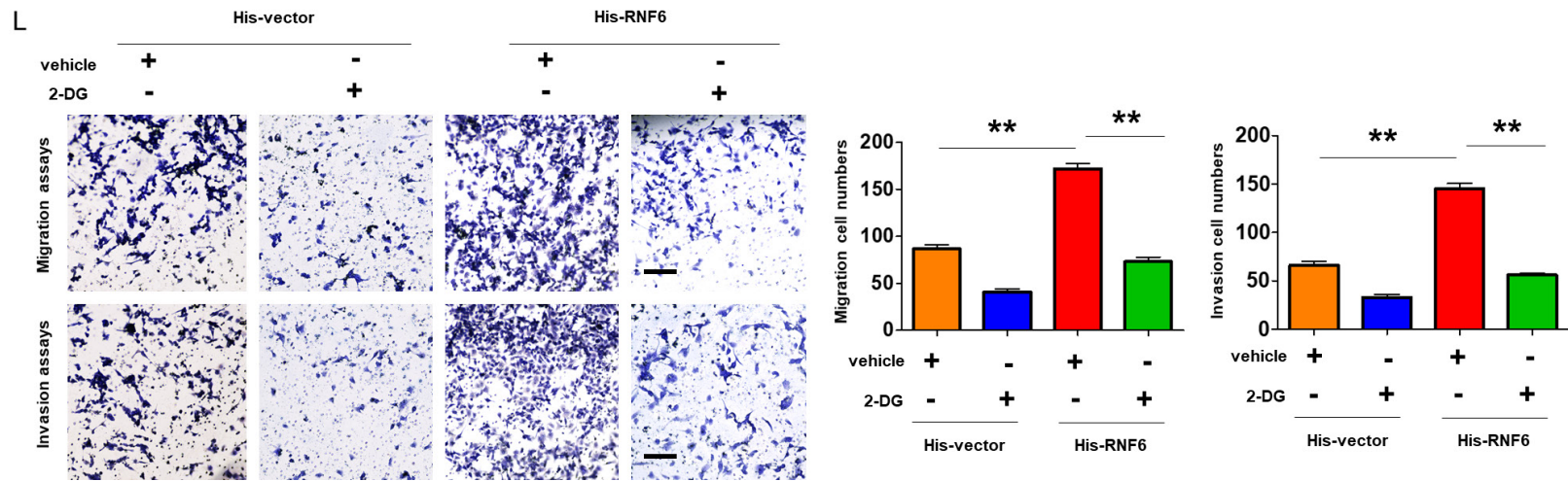


Figure 3. RNF6 promotes migration and invasion of PC cells by modulating Warburg effect. A. KEGG analysis revealed that the top down-regulated gene set in RNF6-silenced cells was associated with glycolysis. B-D. Glucose consumption, lactate production, and ATP levels in AsPC-1/shRNF6 cells. Three independent experiments were performed. $**P < 0.01$. E. ECAR data showing the glycolytic rate and capacity in RNF6-silenced PC cells. Glucose (10 mM), the oxidative phosphorylation inhibitor oligomycin (1.0 μM), and the glycolytic inhibitor 2-deoxyglucose (2-DG, 50 mM) were sequentially injected into each well at the indicated time points. All measurements were normalised to the cell number calculated using a crystal violet assay at the end of the experiment. $**P < 0.01$. F. OCR results showing the basal respiration and maximum respiration in RNF6-silenced PC cells. Oligomycin (1.0 μM), the mitochondrial uncoupler carbonyl cyanide p-trifluoromethoxy phenylhydrazone (FCCP, 1.0 μM), and the mitochondrial complex I inhibitor rotenone plus the mitochondrial complex III inhibitor antimycin A (Rote/AA, 0.5 μM) were sequentially injected. All measurements were normalised to the cell number calculated using crystal violet assay at the end of the experiment. $*P < 0.05$. G-I. Glucose consumption, lactate production, and ATP levels in PANC-1/His-RNF6 cells. $*P < 0.05$, $**P < 0.01$. J. ECAR data showing the glycolytic rate and capacity in RNF6-overexpressing PC cells. $*P < 0.05$. K. OCR results showing the basal respiration and maximum respiration in RNF6-overexpressing PC cells. $*P < 0.05$. L. Effects of 2-DG on the migration and invasion of PANC-1/His-RNF6 cells. The image was captured at 400 \times magnification. Scale bar, 50 μm . $**P < 0.01$.

pression significantly enhanced the glycolysis activity of PANC-1 and CaPan-1 cells (**Figures 3G-K, S3F-J**).

To determine whether the oncogenic role of RNF6 is dependent on the Warburg effect in PC, the glycolytic inhibitor 2-deoxy-D-glucose (2-DG) was used to abolish glycolysis in PANC-1 cells transfected with vectors containing RNF6. As shown in **Figure 3L**, RNF6 overexpression increased the migration and invasion of PANC-1 cell, which was abolished by 2-DG. These findings suggest that RNF6 exerts its oncogenic role by enhancing the Warburg effect in PC.

RNF6 promotes the warburg effect by regulating c-Myc expression in PC

Next, we performed gene set enrichment analysis (GSEA) using the TCGA database to determine the possible associations between RNF6 and c-Myc. As shown in **Figure 4A**, the gene sets of Hallmark_C-MYC_Targets_V1 were obviously enriched in PC samples with high RNF6 level, indicating that c-Myc was closely associated with high RNF6 level in PC. Thus, we speculated that the Warburg effect and metastasis in the RNF6-mediated PC cells might have resulted from elevated levels of c-Myc. As expected, the qRT-PCR data indicated that RNF6 overexpression significantly upregulated c-Myc mRNA expression, whereas RNF6 knock-down suppressed the mRNA level of c-Myc in PC cells (**Figure 4B**). We also found that the protein levels of c-Myc increased in RNF6-overexpression cells, whereas they decreased in RNF6-silenced PC cells (**Figure 4C**). We then investigated the expression of c-Myc target glucose metabolism genes, including glucose transporter *GLUT1*, hexokinase 2 (*HK2*), phosphofruktokinase (*PFKM*) and lactate dehydrogenase A (*LDHA*) in PC cells with RNF6 alteration. As shown in **Figure 4D and 4E**, the mRNA and protein levels of these genes decreased in RNF6-silenced PC cells, whereas the expression of these genes increased in RNF6-overexpression PC cells.

To further determine the correlation between RNF6 and c-Myc, we detected the expression level of c-Myc in PC tissues. As shown in **Figure 4F-H**, the expression level of c-Myc was obviously higher in PC tissues than in normal pancreatic tissues. We also detected the expression level of c-Myc in 36 PC specimens with

high RNF6 expression, using an IHC assay. And, the statistical analysis results indicated that the protein level of c-Myc was positively associated with the protein level of RNF6 in PC tissues (**Figure 4I**). Moreover, as shown in **Figure 4J**, c-Myc overexpression, based on expression in normal pancreatic tissues, occurred in 28 cases (77.8%). Overall, these findings suggest that c-Myc may mediate the regulatory function of RNF6 in PC cells.

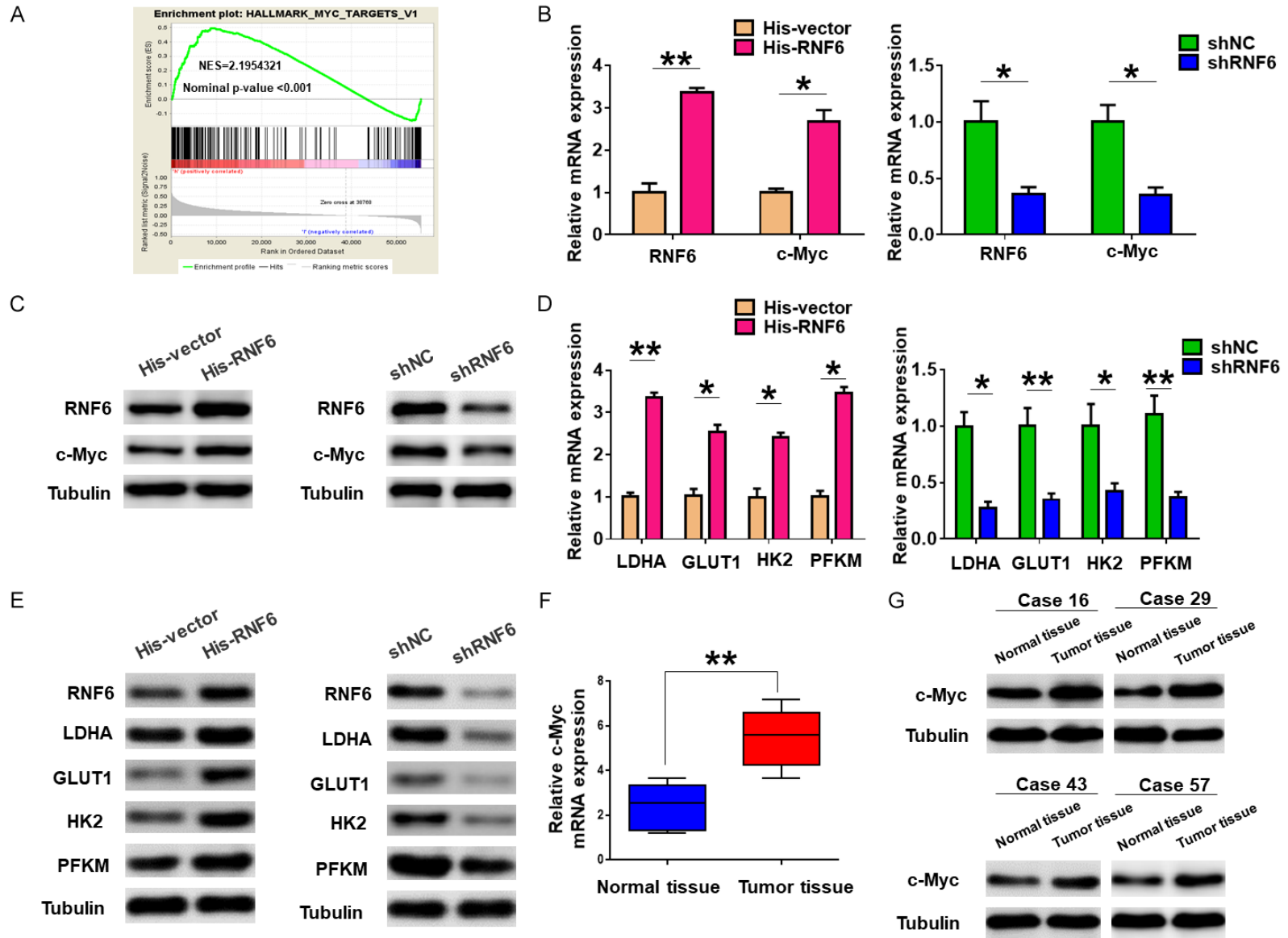
The oncogenic effect of RNF6 in PC is dependent on enhancing c-Myc expression

To investigate whether c-Myc enhancement was responsible for the oncogenic functions of RNF6 in PC, we transfected c-Myc overexpression plasmid into RNF6-knockdown PC cells and examined its effects on these cell biological functions. As shown in **Figure 5A-D**, c-Myc restoration abolished the decrease in glucose uptake, lactate production and ATP generation in RNF6-knockdown PC cells. Additionally, the restored expression of c-Myc also reversed ECAR and OCR loss in RNF6-silenced cells (**Figure 5E and 5F**). Furthermore, the reduction in LDHA, GLUT1, HK2, and PFKM expression in RNF6-silenced cells was also reversed by overexpression of c-Myc (**Figure 5G**). Moreover, the inhibitory effects of RNF6 silencing on migration and invasion were also reversed by c-Myc restoration (**Figure 5H and 5I**). These findings suggest that RNF6 exerts its oncogenic functions by upregulating c-Myc in PC.

RNF6 induces c-Myc expression by downregulating MAD1 expression

To determine how RNF6 modulates c-Myc expression, mass spectrometric analysis was used to identify RNF6-interacting proteins in PC cells. The above results indicate that RNF6 positively regulates the expression of c-Myc in PC cells. As an E3 ubiquitin ligase, RNF6 is responsible for protein degradation and recycling, and we next hypothesized that RNF6 may upregulate c-Myc expression level via degrading the expression of the negative regulator of c-Myc. 35 proteins were identified by mass spectrometry, we found that only the MAD1 (an important cellular antagonist of c-Myc) may interact with RNF6 (**Figure 6A**). Additionally, MAD1 has been linked to the progression of diverse tumors [22, 23]. Further, the data of Co-IP assays confirmed the interaction bet-

RNF6 facilitates pancreatic cancer metastasis



RNF6 facilitates pancreatic cancer metastasis

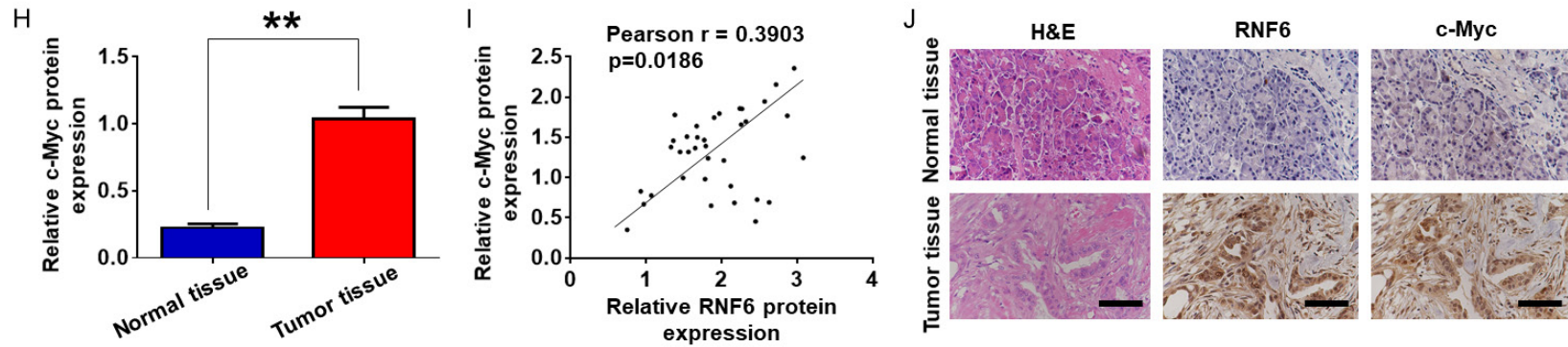


Figure 4. RNF6 promotes glycolysis by regulating c-Myc transcription. A. GSEA comparing the gene sets of Myc targets in RNF6^{high} and RNF6^{low} PC patients. Data were obtained from the TCGA database. NES, normalised enrichment score. B. The mRNA levels of c-Myc in RNF6-overexpressing or RNF6-silenced PC cells were detected by qRT-PCR. * $P < 0.05$, ** $P < 0.01$. C. Protein levels of c-Myc in RNF6-overexpressing or RNF6-silenced PC cells were detected by western blotting. Tubulin was used as a loading control. D. mRNA levels of c-Myc target glucose metabolism genes (LDHA, GLUT1, HK2 and PFKM) in RNF6-overexpressing or RNF6-silenced PC cells were detected by qRT-PCR. * $P < 0.05$, ** $P < 0.01$. E. Protein levels of LDHA, GLUT1, HK2 and PFKM in RNF6-overexpressing or RNF6-silenced PC cells were detected by western blotting. Tubulin was used as a loading control. F. qRT-PCR analysis of c-Myc mRNA expression in PC tumours and paired normal tissues. ** $P < 0.01$. G and H. Determination and quantification of c-Myc protein levels in PC tissues and paired normal tissues by western blotting assay. Tubulin was used as a loading control. I. Scatter plots show a positive correlation between RNF6 and c-Myc at the protein level in PC. J. Representative IHC staining of RNF6 and c-Myc in PC tissues and paired normal tissues. The image was captured at 400 \times magnification. Scale bar, 50 μ m.

RNF6 facilitates pancreatic cancer metastasis

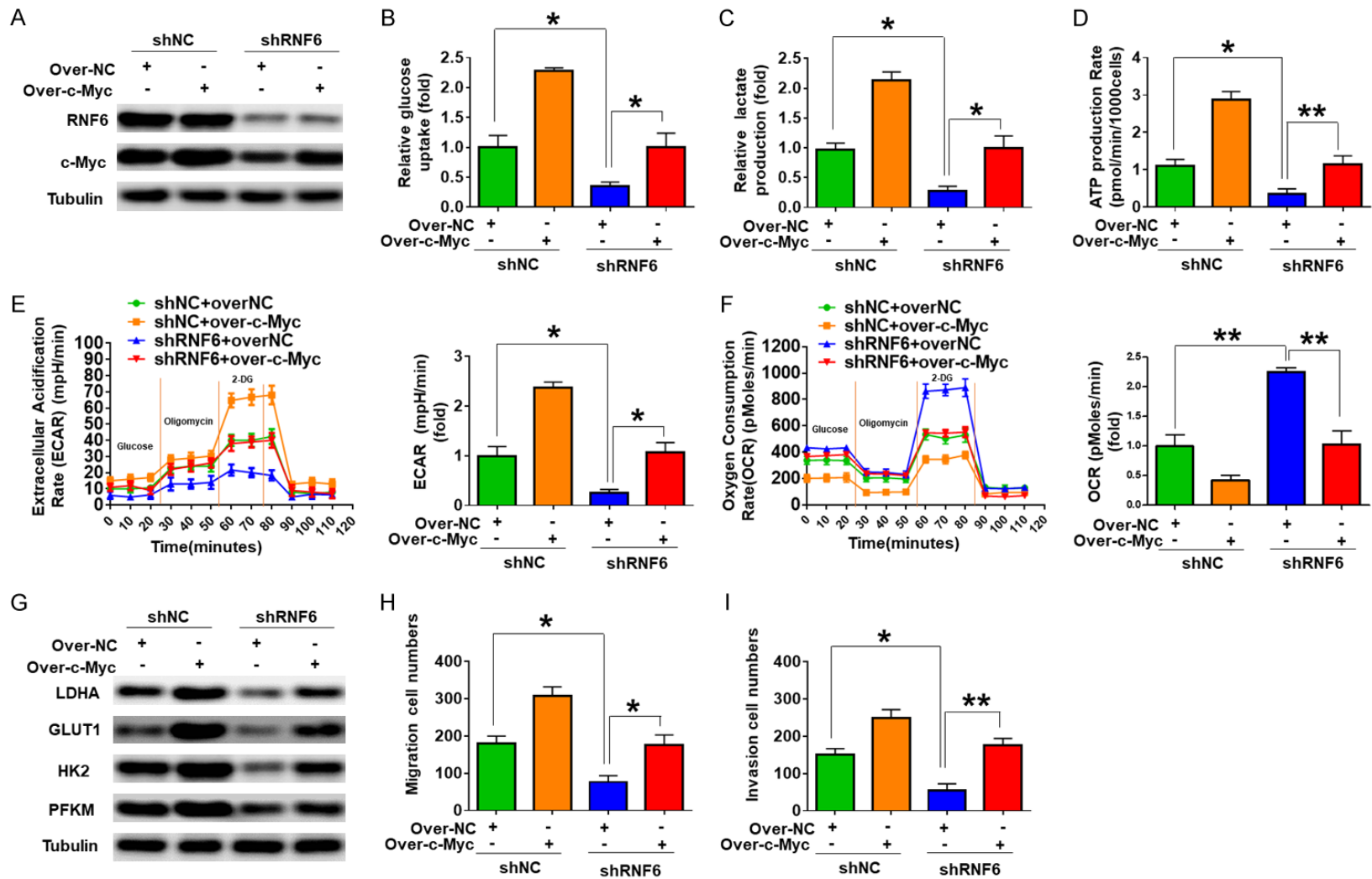


Figure 5. Oncogenic effect of RNF6 is dependent on c-Myc enhancement. A. After overexpression of c-Myc in RNF6 knockdown AsPC-1 cells, the protein levels of RNF6 and c-Myc were detected. Tubulin was used as a loading control. B-D. After overexpression of c-Myc in RNF6-silenced AsPC-1 cells, glucose uptake, the production of lactate and ATP were measured. E and F. After overexpression of c-Myc in RNF6-knockdown AsPC-1 cells, the ECAR and OCR were measured. G. After overexpression of c-Myc in RNF6-silenced AsPC-1 cells, protein levels of LDHA, GLUT1, HK2 and PFKM were detected. Tubulin was used as a loading control. H and I. After overexpression of c-Myc in RNF6-knockdown AsPC-1 cells, cell migration and invasive capacity were measured using the transwell assay. * $P < 0.05$, ** $P < 0.01$.

RNF6 facilitates pancreatic cancer metastasis

direct interaction between RNF6 and MAD1 in HEK293 cells. D and E. Protein levels of RNF6 and MAD1 in RNF6-overexpressing or RNF6-silenced PC cells were detected by western blotting. Tubulin was used as a loading control. F and G. After knockdown of MAD1 in RNF6-silenced PC cells, the protein levels of RNF6, c-Myc and MAD1 were detected. Tubulin was used as a loading control. H and I. After restoration of MAD1 in RNF6-overexpression PC cells, the protein levels of RNF6, c-Myc and MAD1 were detected. Tubulin was used as a loading control.

ween RNF6 and MAD1 in AsPC-1 and PANC-1 cells (**Figure 6B**). Moreover, the GST pull-down assay indicated that RNF6 could bind to MAD1 under cell-free conditions (**Figure 6C**). These results suggested that RNF6 directly interacted with MAD1 in PC cells.

Next, we assessed whether RNF6 could regulate the expression level of MAD1 in PC cells. As shown in **Figure 6D**, RNF6 knockdown obviously upregulated the protein level of MAD1 in AsPC-1 and BxPC-3 cells, whereas RNF6 overexpression significantly reduced the protein level of MAD1 in PANC-1 and CaPan-1 cells (**Figure 6E**). However, the mRNA level of MAD1 was not affected by RNF6 alteration in PC cells (**Figure S4**), indicating that RNF6 regulates the expression of MAD1 via the post-translational modification.

Finally, our findings revealed that RNF6 silencing did not further suppress c-Myc expression in MAD1-silenced PC cells (**Figure 6F and 6G**). Conversely, ectopic expression of MAD1 obviously dampened c-Myc induction in RNF6-overexpression PC cells (**Figure 6H and 6I**). Collectively, these data indicate that MAD1 may be required for the regulatory role of RNF6 on c-Myc expression.

RNF6 mediates ubiquitination and degradation of MAD1

Prior studies have demonstrated that MAD1 can be polyubiquitinated and degraded by the UPS [24]. As an E3 ubiquitin ligase, RNF6 is responsible for protein degradation. Hence, we speculated that RNF6 mediated the reduction in MAD1 levels by modulating the ubiquitination level of MAD1. To test this notion, we first examined the degradation of MAD1 protein following treatment with cycloheximide (CHX). As shown in **Figure 7A and 7B**, RNF6 silencing significantly inhibited the degeneration of MAD1 protein in PC cells. Secondly, we found that the protein level of MAD1 was restored in RNF6-overexpression cells following treatment with the proteasome inhibitor MG132 (**Figure 7C**). Thirdly, RNF6 overexpression increased the

ubiquitination level of MAD1, whereas RNF6 knockdown reduced the poly-ubiquitination level of MAD1 in PC cells (**Figure 7D**). Finally, all Lys mutation in MAD1 could abolish RNF6-mediated MAD1 poly-ubiquitination in PC cells (**Figure 7E**). Furthermore, K48R mutation on Ub almost completely eliminated RNF6-mediated MAD1 poly-ubiquitination, whereas K63R mutation on Ub had no effect (**Figure 7F**). Overall, these findings suggest that RNF6 serves as an E3 ubiquitin ligase responsible for MAD1 degradation via the ubiquitin-proteasome pathway in PC.

Discussion

RNF6, a main member of the RING finger E3 ligase family, has been shown to play critical roles in tumorigenesis in several types of cancers [15, 18, 25]. However, there is currently no information on the role and mechanism of RNF6 in PC. In this study, we found that RNF6 was highly expressed in PC tissues, and an increased in RNF6 expression was closely associated with malignant phenotype of patients with PC. In addition, we examined the role of RNF6 in PC tumorigenesis using cell culture approaches and animal-based tumour models. We found that RNF6 promotes PC cell migration and invasion *in vitro*, and metastasis *in vivo*, thereby implying that *RNF6* may serve as an oncogene in PC. We believe, to the best of our knowledge, that this is the first study to explore the role of RNF6 in PC.

The Warburg effect, a hallmark of cancer cells, is a crucial process during cancer metastasis. Therefore, understanding the potential regulatory mechanisms of the Warburg effect in PC will be beneficial for the prevention and treatment of this malignant cancer. In the process of the Warburg effect, c-Myc plays a critical role through directly regulating the expression of glycolytic enzyme-related genes [9, 26]. Our GSEA data suggested that the c-Myc target genes were closely associated with high RNF6 level in PC tissues. Hence, we attempted to investigate whether the pro-tumour role of

RNF6 facilitates pancreatic cancer metastasis

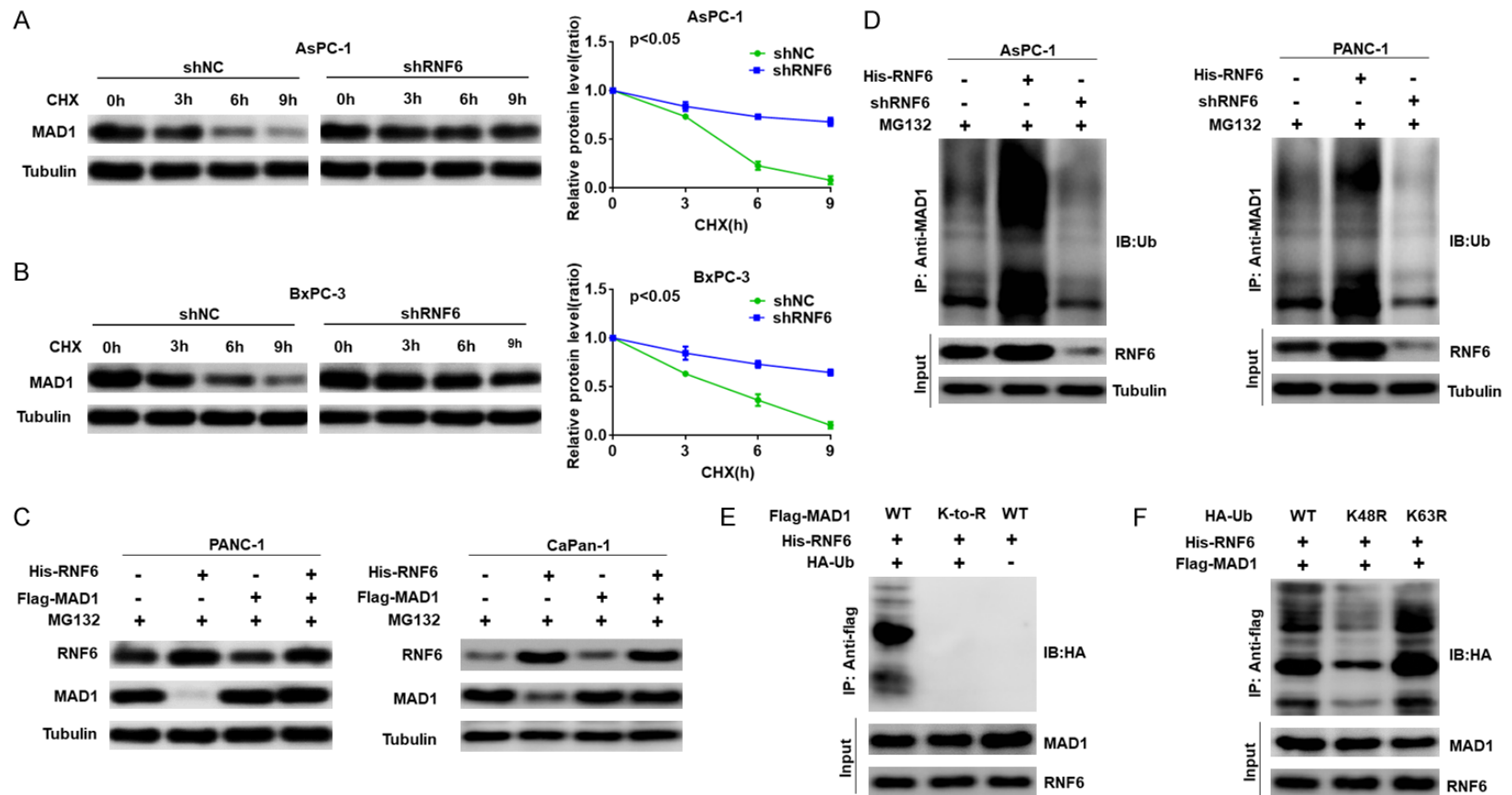


Figure 7. RNF6 destabilises MAD1 by promoting MAD1 ubiquitination and degradation in PC cells. A and B. Representative western blot showing that RNF6 knock-down promotes degeneration of MAD1 protein in PC cells. PC cells were treated with cycloheximide (CHX, 100 mg/ml) for indicated time points and subjected to western blot analysis (left); the quantitative results of MAD1 protein level determination are shown (right). C. PC cells transfected with His-RNF6 were treated with 10 μ M MG132. Cells were collected at 6 h and immunoblotted with the antibodies indicated. D. Knockdown or exogenous expression of RNF6 altered the ubiquitination of MAD1. The cells in each group were treated with proteasomal inhibitor MG132. Cell lysates were prepared and subjected to immunoprecipitation with anti-MAD1 antibodies. The level of ubiquitin-attached MAD1 was detected by western blotting with anti-Ub antibodies. E. Ubiquitination of wild-type MAD1 or the K-to-R mutant (mutations in all Lys site of *MAD1* gene) in HEK293 cells. F. Determination of MAD1 ubiquitination type in HEK293 cells.

RNF6 facilitates pancreatic cancer metastasis

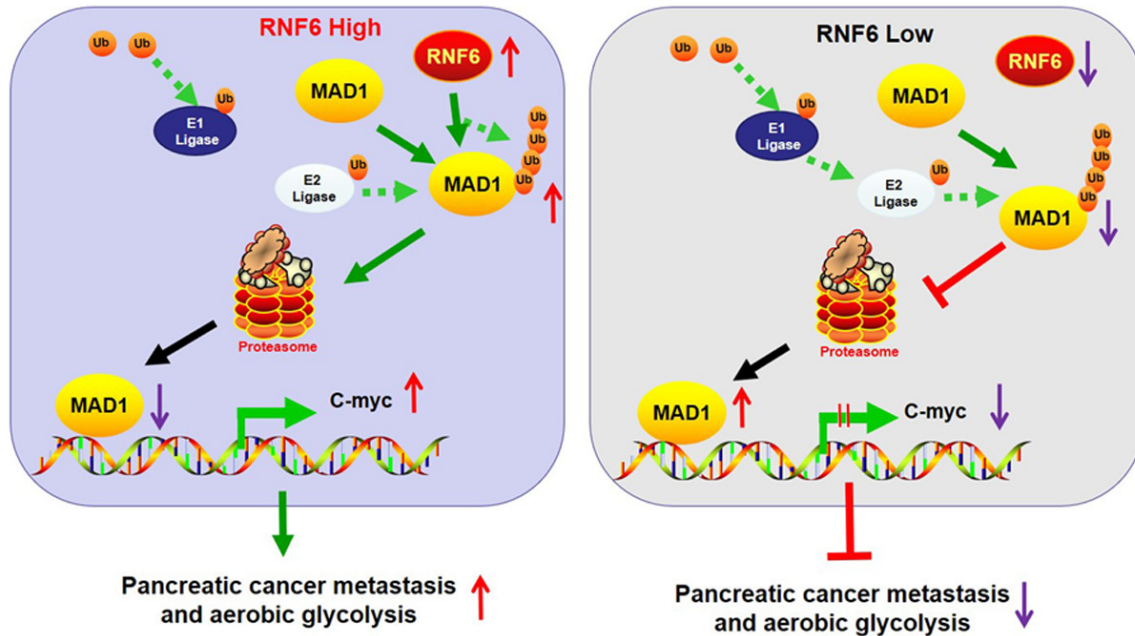


Figure 8. Proposed model by which E3 ubiquitin ligase RNF6 promotes pancreatic cancer metastasis by enhancing c-Myc-mediated Warburg effect via destabilization of MAD1.

RNF6 was dependent on the c-Myc mediated Warburg effect. Indeed, RNF6 silencing significantly suppressed the expression of c-Myc as well as the metabolic phenotype of aerobic glycolysis. In contrast, RNF6 overexpression dramatically enhanced the glycolytic activity of PC cells. Importantly, ectopic expression of c-Myc could abolish the reduced glycolysis and malignant phenotypes in RNF6-silenced PC cells, indicating that RNF6 exerted its oncogenic function via the c-Myc-mediated Warburg effect.

It is well known that the regulation mechanism of c-Myc is very complex. Ectopic expression of c-Myc in many cancers is caused by genetic amplifications, insertions, and translocations [27, 28]. Various factors such as TIP30 [29], microRNA 145 [30], Fbxw7 [31] and SKP2 [32] can regulate c-Myc expression via transcriptional, post-transcriptional mechanisms and post-translational modifications. In the present study, we clarified the mechanisms by which RNF6 mediates the overexpression of c-Myc in PC. RNF6 may upregulate the expression of c-Myc by ubiquitinating and degrading MAD1, but not other regulators of c-Myc. Our data indicate that RNF6 alteration could regulate the expression level of c-Myc and its transcriptional

repressor MAD1. Importantly, Mass spectrometry and Co-IP assay showed that RNF6 did not interact with c-Myc (Figure S5) but interacted with the MAD1 in PC cells. These results suggest that RNF6 indirectly upregulates c-Myc expression by disrupting MAD1 expression.

Studies have shown that MAD1 is a key negative regulator of c-Myc [33]. Moreover, the UPS-mediated degradation of MAD1 is an important mechanism for regulating the expression level of MAD1 in many cancers [34, 35]. Consistent with these results, we found that RNF6 is involved in the MAD1 degradation process and serves as an E3 ubiquitin ligase for MAD1 in PC cells. This notion is supported by three lines of experimental evidence. First, RNF6 can decrease the half-life of MAD1. Second, treatment with MG132, a proteasome inhibitor, abolishes RNF6-induced MAD1 degradation in PC cells. Third, RNF6 silencing decreases the ubiquitination levels of MAD1, whereas RNF6 overexpression increase them.

In conclusion, we found that RNF6 interacted with MAD1 and increased its poly-ubiquitination level, thereby destabilising MAD1 and causing the activation of the c-Myc-mediated Warburg effect in PC (Figure 8). Additionally, a

high RNF6 level was significantly associated with a poor outcome for patients with PC. Mechanistically, our results demonstrate that RNF6 contributes to PC metastasis by enhancing the MAD1/c-Myc axis-mediated Warburg effect, thus suggesting that targeting RNF6/MAD1/c-Myc axis is a potential strategy for PC therapy.

Acknowledgements

This study was supported by grants from the National Natural Science Foundation of China (No. 81760523, No. 81560117 and No. 360-60166), the China Postdoctoral Science Foundation (2016M590607), the Jiangxi Provincial Postdoctoral Science Foundation (2016KY24), the Project of the Jiangxi Provincial Department of Science and Technology (20202AC-BL216002, No. 20192BAB205024 and No. 20202ACBL216013).

Disclosure of conflict of interest

None.

Address correspondence to: Xiaogang Peng, Jiangxi Province Key Laboratory of Molecular Medicine, The Second Affiliated Hospital of Nanchang University, No. 1 Minde Road, Nanchang 330006, Jiangxi Province, China. Tel: +86-791-86297662; Fax: +86-791-86297662; E-mail: pxg8205@163.com; Leifeng Chen, Department of General Surgery, The Second Affiliated Hospital of Nanchang University, No. 1 Minde Road, Nanchang 330006, Jiangxi Province, China. E-mail: 18770099029@126.com; Mingfeng Xiang, Department of Urology, The Second Affiliated Hospital of Nanchang University, Nanchang 330006, Jiangxi Province, China. E-mail: xmf6686@163.com

References

- [1] Siegel RL, Miller KD and Jemal A. Cancer statistics, 2019. *CA Cancer J Clin* 2019; 69: 7-34.
- [2] McGuigan A, Kelly P, Turkington RC, Jones C, Coleman HG and McCain RS. Pancreatic cancer: a review of clinical diagnosis, epidemiology, treatment and outcomes. *World J Gastroenterol* 2018; 24: 4846-4861.
- [3] Crippa S, Angelini C, Mussi C, Bonardi C, Romano F, Sartori P, Uggeri F and Bovo G. Surgical treatment of metastatic tumors to the pancreas: a single center experience and review of the literature. *World J Surg* 2006; 30: 1536-1542.
- [4] Ren B, Cui M, Yang G, Wang H, Feng M, You L and Zhao Y. Tumor microenvironment participates in metastasis of pancreatic cancer. *Mol Cancer* 2018; 7: 108.
- [5] Vaupel P, Schmidberger H and Mayer A. The Warburg effect: essential part of metabolic reprogramming and central contributor to cancer progression. *Int J Radiat Biol* 2019; 95: 912-919.
- [6] Cui J, Shi M, Xie D, Wei D, Jia Z, Zheng S, Gao Y, Huang S and Xie K. FOXM1 promotes the Warburg effect and pancreatic cancer progression via transactivation of LDHA expression. *Clin Cancer Res* 2014; 20: 2595-2606.
- [7] Yang J, Ren B, Yang G, Wang H, Chen G, You L, Zhang T and Zhao Y. The enhancement of glycolysis regulates pancreatic cancer metastasis. *Cell Mol Life Sci* 2020; 77: 305-321.
- [8] Dang CV. MYC on the path to cancer. *Cell* 2012; 149: 22-35.
- [9] Dang CV, Le A and Gao P. MYC-induced cancer cell energy metabolism and therapeutic opportunities. *Clin Cancer Res* 2009; 15: 6479-6483.
- [10] Gabay M, Li Y and Felsher DW. MYC activation is a hallmark of cancer initiation and maintenance. *Cold Spring Harb Perspect Med* 2014; 4: a014241.
- [11] Wirth M, Mahboobi S, Krämer OH and Schneider G. Concepts to target MYC in pancreatic cancer. *Mol Cancer Ther* 2016; 15: 1792-1798.
- [12] Sun Y. Targeting E3 ubiquitin ligases for cancer therapy. *Cancer Biol Ther* 2003; 2: 623-629.
- [13] Xu K, Shimelis H, Linn DE, Jiang R, Yang X, Sun F, Guo Z, Chen H, Li W, Chen H, Kong X, Melamed J, Fang S, Xiao Z, Veenstra TD and Qiu Y. Regulation of androgen receptor transcriptional activity and specificity by RNF6-induced ubiquitination. *Cancer Cell* 2009; 15: 270-282.
- [14] Tursun B, Schlüter A, Peters MA, Viehweger B, Ostendorff HP, Soosairajah J, Drung A, Bossenz M, Johnsen SA, Schweizer M, Bernard O and Bach I. The ubiquitin ligase Rnf6 regulates local LIM kinase 1 levels in axonal growth cones. *Genes Dev* 2005; 19: 2307-2319.
- [15] Cai J, Xiong Q, Jiang X, Zhou S and Liu T. RNF6 facilitates metastasis and radioresistance in hepatocellular carcinoma through ubiquitination of FoxA1. *Exp Cell Res* 2019; 374: 152-161.
- [16] Lo HS, Hu N, Gere S, Lu N, Su H, Goldstein AM, Taylor PR and Lee MP. Identification of somatic mutations of the RNF6 gene in human esophageal squamous cell carcinoma. *Cancer Res* 2002; 62: 4191-4193.
- [17] Heemers HV and Tindall DJ. Unraveling the complexities of androgen receptor signaling in

- prostate cancer cells. *Cancer Cell* 2009; 15: 245-247.
- [18] Liang Q, Ma D, Zhu X, Wang Z, Sun TT, Shen C, Yan T, Tian X, Yu T, Guo F, Tang J, Lin Y, Chen H, Zhou C, Ge Z, Zhong M, Chen J, Liu Q, Wang Z, Fang JY, Chen H and Hong J. RING-finger protein 6 amplification activates JAK/STAT3 pathway by modifying SHP-1 ubiquitylation and associates with poor outcome in colorectal cancer. *Clin Cancer Res* 2018; 24: 1473-1485.
- [19] Liu L, Zhang Y, Wong CC, Zhang J, Dong Y, Li X, Kang W, Chan FKL, Sung JY and Yu J. RNF6 promotes colorectal cancer by activating the wnt/ β -catenin pathway via ubiquitination of TLE3. *Cancer Res* 2018; 78: 1958-1971.
- [20] Lüscher B. MAD1 and its life as a MYC antagonist: an update. *Eur J Cell Biol* 2012; 91: 506-514.
- [21] Lim SO, Li CW, Xia W, Cha JH, Chan LC, Wu Y, Chang SS, Lin WC, Hsu JM, Hsu YH, Kim T, Chang WC, Hsu JL, Yamaguchi H, Ding Q, Wang Y, Yang Y, Chen CH, Sahin AA, Yu D, Hortobagyi GN and Hung MC. Deubiquitination and Stabilization of PD-L1 by CSN5. *Cancer Cell* 2016; 30: 925-939.
- [22] Cao L, Xu C, Xiang G, Liu F, Liu X, Li C, Liu J, Meng Q, Jiao J and Niu Y. AR-PDEF pathway promotes tumour proliferation and upregulates MYC-mediated gene transcription by promoting MAD1 degradation in ER-negative breast cancer. *Mol Cancer* 2018; 17: 136.
- [23] Wang HB, Wang XW, Zhou G, Wang WQ, Sun YG, Yang SM and Fang DC. PinX1 inhibits telomerase activity in gastric cancer cells through Mad1/c-Myc pathway. *J Gastrointest Surg* 2010; 14: 1227-1234.
- [24] Li H, Fang Y, Niu C, Cao H, Mi T, Zhu H, Yuan J and Zhu J. Inhibition of cIAP1 as a strategy for targeting c-MYC-driven oncogenic activity. *Proc Natl Acad Sci U S A* 2018; 115: E9317-E9324.
- [25] Lipkowitz S and Weissman AM. RINGS of good and evil: RING finger ubiquitin ligases at the crossroads of tumour suppression and oncogenesis. *Nat Rev Cancer* 2011; 11: 629-643.
- [26] Luo P, Zhang C, Liao F, Chen L, Liu Z, Long L, Jiang Z, Wang Y, Wang Z, Liu Z, Miao H and Shi C. Transcriptional positive cofactor 4 promotes breast cancer proliferation and metastasis through c-Myc mediated Warburg effect. *Cell Commun Signal* 2019; 17: 36.
- [27] Beroukhi R, Mermel CH, Porter D, Wei G, Raychaudhuri S, Donovan J, Barretina J, Boehm JS, Dobson J, Urashima M, Mc Henry KT, Pinchback RM, Ligon AH, Cho YJ, Haery L, Greulich H, Reich M, Winckler W, Lawrence MS, Weir BA, Tanaka KE, Chiang DY, Bass AJ, Loo A, Hoffman C, Prensner J, Liefeld T, Gao Q, Yecies D, Signoretti S, Maher E, Kaye FJ, Sasaki H, Tepper JE, Fletcher JA, Tabernero J, Baselga J, Tsao MS, Demichelis F, Rubin MA, Janne PA, Daly MJ, Nucera C, Levine RL, Ebert BL, Gabriel S, Rustgi AK, Antonescu CR, Ladanyi M, Letai A, Garraway LA, Loda M, Beer DG, True LD, Okamoto A, Pomeroy SL, Singer S, Golub TR, Lander ES, Getz G, Sellers WR and Meyer-son M. The landscape of somatic copy-number alteration across human cancers. *Nature* 2010; 463: 899-905.
- [28] Niitsu N, Okamoto M, Miura I and Hirano M. Clinical features and prognosis of de novo diffuse large B-cell lymphoma with t(14;18) and 8q24/c-MYC translocations. *Leukemia* 2009; 23: 777-783.
- [29] Jiang C, Ito M, Piening V, Bruck K, Roeder RG and Xiao H. TIP30 interacts with an estrogen receptor alpha-interacting coactivator CIA and regulates c-myc transcription. *J Biol Chem* 2004; 279: 27781-27789.
- [30] Sachdeva M, Zhu S, Wu F, Wu H, Walia V, Kumar S, Elble R, Watabe K and Mo YY. p53 represses c-Myc through induction of the tumor suppressor miR-145. *Proc Natl Acad Sci U S A* 2009; 106: 3207-3212.
- [31] Welcker M, Orian A, Jin J, Grim JE, Harper JW, Eisenman RN and Clurman BE. The Fbw7 tumor suppressor regulates glycogen synthase kinase 3 phosphorylation-dependent c-Myc protein degradation. *Proc Natl Acad Sci U S A* 2004; 101: 9085-9090.
- [32] von der Lehr N, Johansson S, Wu S, Bahram F, Castell A, Cetinkaya C, Hydbring P, Weidung I, Nakayama K, Nakayama KI, Söderberg O, Kerppola TK and Larsson LG. The F-box protein Skp2 participates in c-Myc proteasomal degradation and acts as a cofactor for c-Myc-regulated transcription. *Mol Cell* 2003; 11: 1189-1200.
- [33] McArthur GA, Foley KP, Fero ML, Walkley CR, Deans AJ, Roberts JM and Eisenman RN. MAD1 and p27(KIP1) cooperate to promote terminal differentiation of granulocytes and to inhibit Myc expression and cyclin E-CDK2 activity. *Mol Cell Biol* 2002; 22: 3014-3023.
- [34] Xu L, Zhu J, Hu X, Zhu H, Kim HT, LaBaer J, Goldberg A and Yuan J. c-IAP1 cooperates with Myc by acting as a ubiquitin ligase for Mad1. *Mol Cell* 2007; 28: 914-922.
- [35] Zhu J, Blenis J and Yuan J. Activation of PI3K/Akt and MAPK pathways regulates Myc-mediated transcription by phosphorylating and promoting the degradation of Mad1. *Proc Natl Acad Sci U S A* 2008; 105: 6584-6589.

RNF6 facilitates pancreatic cancer metastasis

Supplementary methods

Cell lines and cell culture

Four PC cell lines (AsPC-1, BxPC-3, PANC-1 and CaPan-1) and the normal pancreatic ductal epithelial cell line (H6C7) were purchased from American Type Culture Collection (Manassas, VA, USA). The cell lines were cultured in Dulbecco's Modified Eagle's Medium (Gibco, USA) supplemented with 10% fetal bovine serum and 100 units/mL of penicillin-streptomycin (Invitrogen, USA) at 37°C in a humidified atmosphere containing 5% CO₂.

Quantitative real-time (qRT)-PCR

Total RNA was isolated from cells using Trizol reagent (Invitrogen, USA). qRT-PCR was performed using SYBR Green qPCR Master Mix (Clontech Laboratories, USA) with Applied Biosystems® 7900HT Fast real-Time PCR System system (Thermo Fisher Scientific, USA). The primers used are listed in the following table.

RNF6 forward	5'-CAAGACCTGGAGAGATGGGCAG-3'
RNF6 reverses	5'-GATTCATCCTGAGATTCCTGGCT-3'
MAD1 forward	5'-TGGAGAAGAATAGACGGGCT-3'
MAD1 reverses	5'-GCTGGTCGATTTGGTGAACG-3'
c-Myc forward	5'-TACAACACCCGAGCAAGGAC-3'
c-Myc reverses	5'-CTAACGTTGAGGGGCATCGT-3'
LDHA forward	5'-CATGGCCTGTGCCATCAGTA-3'
LDHA reverses	5'-AGATATCCACTTTGCCAGAGACA-3'
HK2 forward	5'-CAGCACAAGCAGTCGGACC-3'
HK2 reverses	5'-CAGAGAGGCGCATGTGGTAG-3'
PFKM forward	5'-GGAGAAACAGCCAAAGGGGA-3'
PFKM reverses	5'-GGAGAAACAGCCAAAGGGGA-3'
GLUT1 forward	5'-TTGGCTCCGGTATCGTCAAC-3'
GLUT1 reverses	5'-GGCCACGATGCTCAGATAGG-3'
GAPDH forward	5'-GTTAGGAAAGCCTGCCGGTG-3'
GAPDH reverses	5'-GAGTTAAAAGCAGCCCTGGTG-3'

Western blot and immunohistochemistry (IHC) assay

For Western blot assay, equal amounts of cell lysates were resolved by SDS/PAGE, electrotransferred to polyvinylidene fluoride (Millipore, USA) membranes and blocked in 5% skim milk. Membranes were immunoblotted with the indicated primary antibodies. Immunoreactive bands were visualized with chemiluminescence kits chemiluminescence (Pierce, USA). The following antibodies were used: antibodies against RNF6 (1:1,000, abcam), c-Myc (1:1,000, abcam), MAD1 (1:1,000, Cell Signaling), LDHA (1:1,000, abcam), GLUT1 (1:1,000, abcam), HK2 (1:1,000, Cell Signaling), PFKM (1:1,000, abcam), ubiquitin (1:1,000, Enzo Life Sciences) and Tubulin (1:1,000, abcam).

For IHC staining, the matched cancerous and normal pancreatic tissue samples were fixed, embedded, sectioned, and deparaffinized. Then, the sections were blocked using serum-free protein block buffer (DAKO, USA) for 30 min, after which they were incubated with anti-RNF6 (1:200, abcam) and anti-c-Myc (1:200, abcam).

Cell migration and invasion assay

The migration/invasion ability of PC cells was routinely examined in a Transwell Boyden Chamber (BD Biosciences, USA). For the cell invasion assay, the polycarbonate membranes of the upper compartment of the chambers were pre-coated with a matrix gel.

RNF6 facilitates pancreatic cancer metastasis

GST pull-down assay

GST-RNF6 or control GST (Genepharma Company, Shanghai, China) was added into the cell lysates harvested from the cells transfected with Flag-tagged MAD1. After being incubated with Glutathione beads (Sigma-Aldrich, St. Louis, MO, USA) for 2 h, the bound proteins were subjected to western blot analysis using Flag antibodies. For endogenous immunoprecipitation, after being incubated with immunoglobulin G as a control, cell lysates were incubated with protein A beads (Sigma-Aldrich). The bound proteins were used for western blot with RNF6 antibody.

RNF6 facilitates pancreatic cancer metastasis

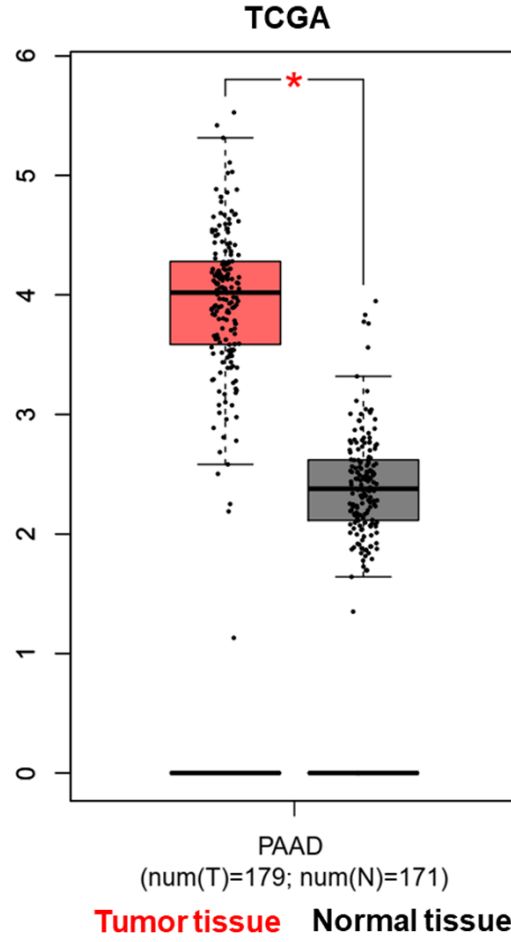


Figure S1. The mRNA level of RNF6 was upregulated in pancreatic cancer tissues via the Cancer Genome Atlas (TCGA) dataset.

RNF6 facilitates pancreatic cancer metastasis

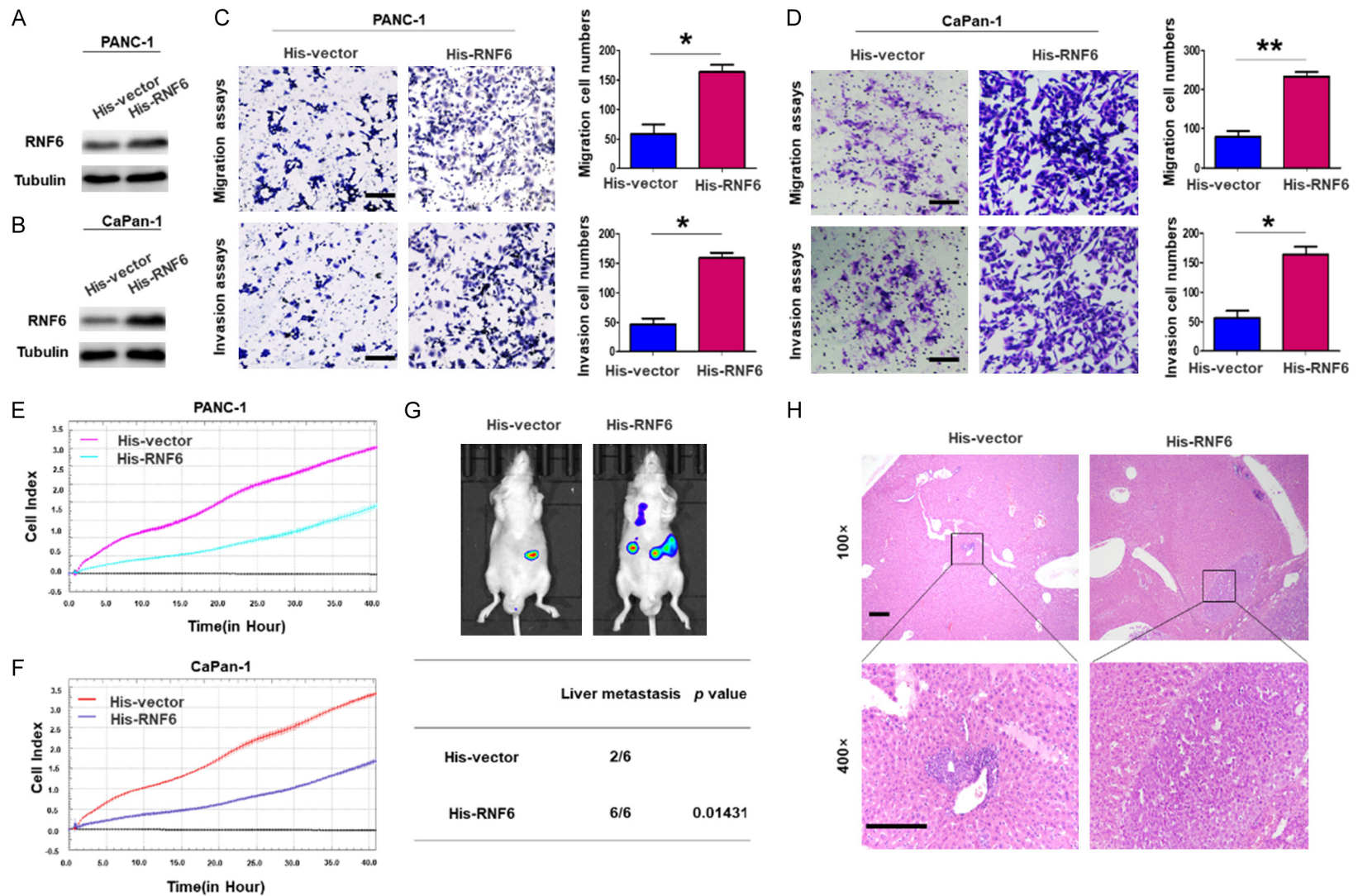


Figure S2. Effects of RNF6 on PC cell metastasis. A and B. Western blot analyses were used to detect the expression level of RNF6 in PANC-1 and CaPan-1 cells stably transfected with the RNF6-overexpression vector. Tubulin was used as a loading control. C and D. Transwell migration and Transwell invasion assays of PANC-1 and CaPan-1 cells transfected with RNF6 overexpression vector. The image was captured at 400× magnification. Scale bar, 50 μm. *P<0.05, **P<0.01. E and F. RTCA assays were performed to detect the metastasis ability of PANC-1 and CaPan-1 cells transfected with RNF6 overexpression vector. G. PANC-1/His-RNF6 cells were injected into the tail vein of nude mice, and the incidence of liver metastasis were measured after 6-8 weeks. n=6, *P<0.05. H. Representative images (left; magnification ×100, inset magnification ×400) and quantification (right) of H&E staining of liver metastatic nodules. n=6/group. Scale bar, 50 μm. **P<0.01.

RNF6 facilitates pancreatic cancer metastasis

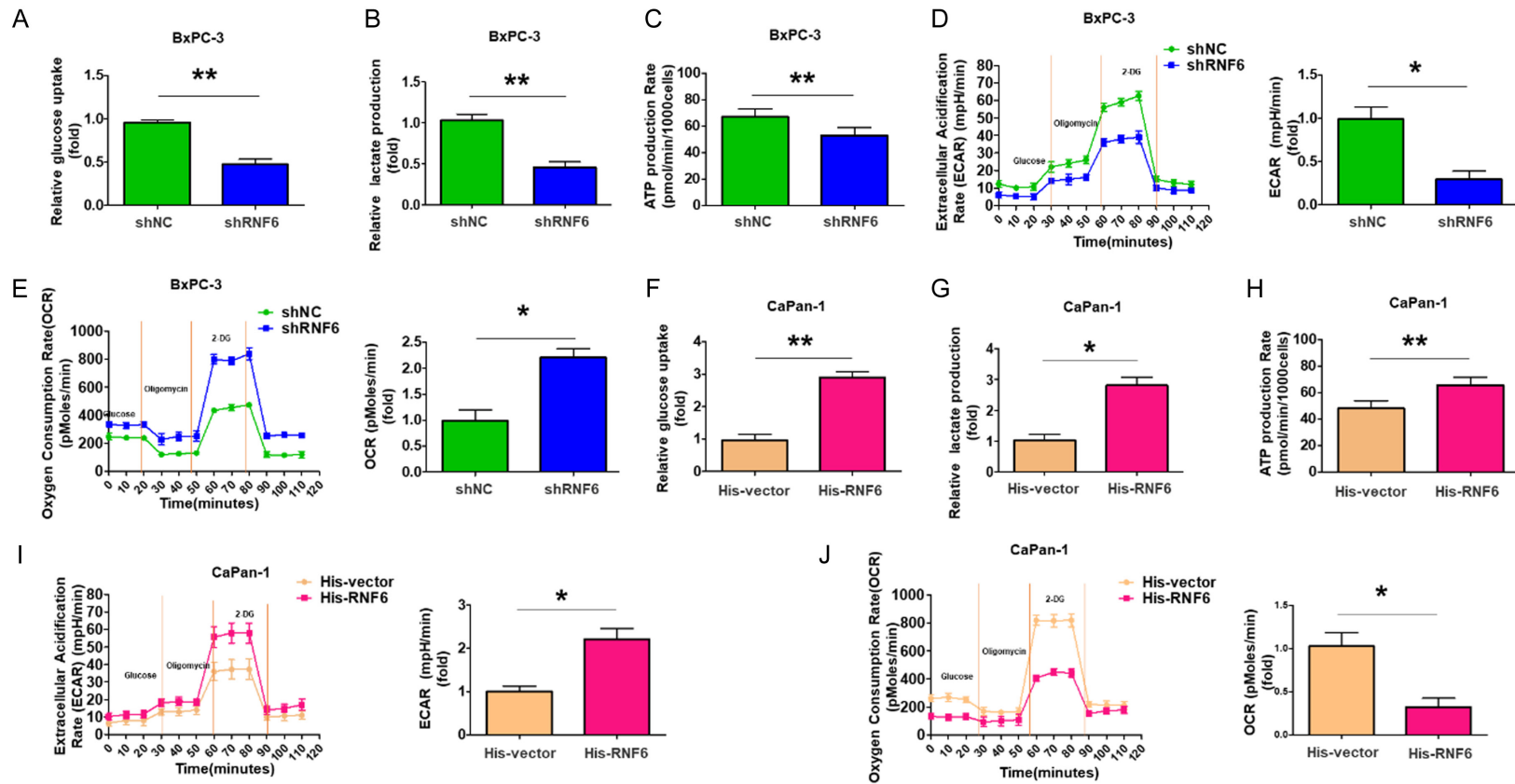


Figure S3. Glycolysis is critically involved in the oncogenic functional of RNF6. A-C. Glucose consumption, lactate production, and ATP levels in BxPC-3/shRNF6 cells. Three independent experiments were performed. ** $P < 0.01$. D. ECAR data showing the glycolytic rate and capacity in RNF6-silenced PC cells. Glucose (10 mM), the oxidative phosphorylation inhibitor oligomycin (1.0 μ M), and the glycolytic inhibitor 2-deoxyglucose (2-DG, 50 mM) were sequentially injected into each well at the indicated time points. All measurements were normalized to the cell number calculated using crystal violet assay at the end of the experiment. * $P < 0.05$. E. OCR results showing the basal respiration and maximum respiration in RNF6-silenced PC cells. Oligomycin (1.0 μ M), the mitochondrial uncoupler carbonyl cyanide p-trifluoromethoxy phenylhydrazone (FCCP, 1.0 μ M), and the mitochondrial complex I inhibitor rotenone plus the mitochondrial complex III inhibitor antimycin A (Rote/AA, 0.5 μ M) were sequentially injected. All measurements were normalized to the cell number calculated using crystal violet assay at the end of the experiment. * $P < 0.05$. F-H. Glucose consumption, lactate production, and ATP levels in CaPan-1/His-RNF6 cells. * $P < 0.05$, ** $P < 0.01$. I. ECAR data showing the glycolytic rate and capacity in RNF6-overexpressing PC cells. * $P < 0.05$. J. OCR results showing the basal respiration and maximum respiration in RNF6-overexpressing PC cells. * $P < 0.05$.

RNF6 facilitates pancreatic cancer metastasis

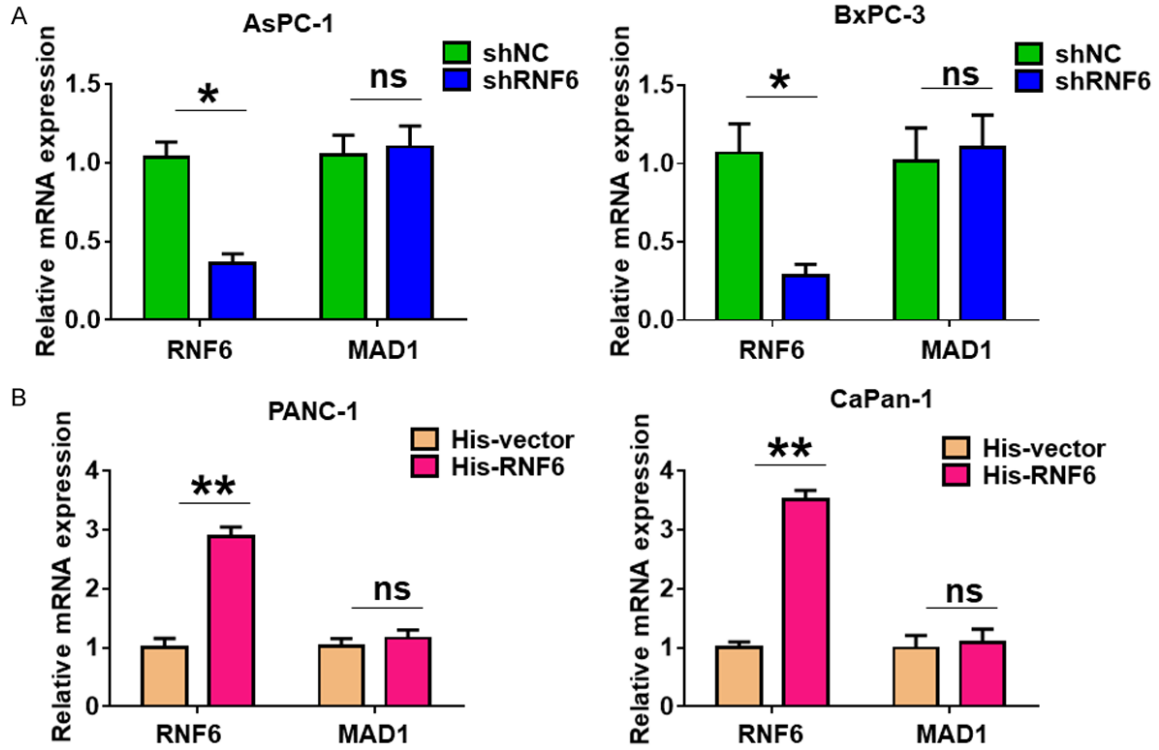


Figure S4. The mRNA level of MAD1 was not affected by RNF6 alteration in PC cells. A. The mRNA levels of RNF6 and MAD1 in RNF6-silenced PC cells were detected by qRT-PCR. $*P < 0.05$. B. The mRNA levels of RNF6 and MAD1 in RNF6-overexpressing PC cells were detected by qRT-PCR. $*P < 0.05$.

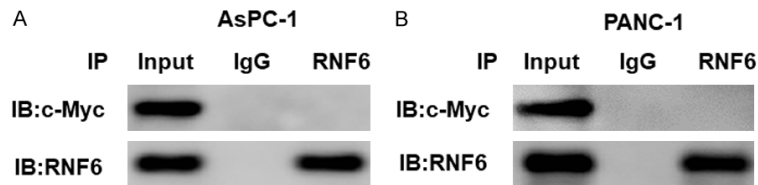


Figure S5. Co-IP assay showing that endogenous RNF6 and c-Myc were not directly bound.